

<https://doi.org/10.1038/s43856-025-00822-w>

Potential influence of geomagnetic activity on blood pressure statistical fluctuations at mid-magnetic latitudes

Check for updates

Pengzhi He^{1,13}, Chen Li^{2,13}, Minlan Xu³, Ruilong Guo¹, Alexander William Degeling¹, Timo Pitkänen¹, Yude Bu⁴, Xiangyun Zheng⁵, Yue Zhang⁵, Xianghong Jia¹, Anmin Tian¹, Chenyao Han¹, Shifeng Wang⁶, Tianlu Chen⁷, Jiangping Fang⁸, Shaowei Sun⁵, Wenlong Liu⁹, Jinbin Cao⁹, Kimmen Quan¹⁰, Zhiyuan Cong⁸, Dedong Ma¹¹, Qiugang Zong¹², Suiyan Fu¹², Shutao Yao¹, Huanhu Zhang¹³✉ & Quanqi Shi¹✉

Abstract

Background Solar activity and the consequent geomagnetic activity (GMA) profoundly influence human biological rhythms and cardiovascular system functions. Although the response of blood pressure (BP) to GMA has attracted considerable attention, it is unclear whether the GMA can have an influence alone and how it occurs.

Methods In this six-year time series analysis, we collated over 500,000 BP measurements from two representative cities (Qingdao and Weihai) at mid-magnetic latitudes in China. Using various statistical methods, we analyzed the correlation between BP and the GMA (represented by Ap index) and their quasi-periodic fluctuations. Additionally, we conducted a comparative analysis of the influence of other environmental factors (air temperature and PM2.5) on BP.

Results The statistical BP level fluctuations correlate with the GMA. Both BP and the GMA index exhibit similar annual bimodal patterns and multiple periodicities, including 12-month and 6-month cycles, and an intermittent 3-month cycle. In contrast, other known environmental factors influencing BP such as air temperature and PM2.5 do not exhibit similar periodicities, particularly they lack 3-month cycles. In years with higher GMA levels, the BP shows stronger correlations with the Ap index and responds on a shorter timescale. Additionally, BP in females appears to be more strongly correlated with GMA.

Conclusions Our findings highlight potential risks to individuals with hypertension with elevated GMA levels, deepen our understanding of GMA's role in human health, and offer insights for healthcare policymakers on the clinical significance of the geomagnetic environment.

Plain Language Summary

Human blood pressure fluctuates constantly and is influenced by various factors such as hormone levels in the body and environmental conditions. Geomagnetic activity is change in the Earth's magnetic field as a consequence of the sun's activity, such as the impact of solar winds. We used six years of data to investigate whether changes in geomagnetic activity have an impact on blood pressure. Our results show a relationship between geomagnetic activity and blood pressure, particularly during periods of high geomagnetic activity. Understanding this relationship could enhance our knowledge of the geomagnetic environment's clinical significance and potentially contribute to better hypertension risk assessment and management.

Hypertension is a widespread and highly consequential cardiovascular disease. It substantially increases the likelihood of developing various disorders affecting the heart, brain, kidneys, and other vital organs. Therefore, enhancing our scientific understanding of the causes of hypertension is crucial for early detection and timely intervention.

Numerous previous studies have investigated environmental factors such as air temperature and air pollutants on earth, particularly particulate matter with an aerodynamic diameter less than 2.5 microns (PM2.5), highlighting their significant effects on BP^{1–3}. But in the Sun-Earth system, research into the effects of solar activity and the consequent GMA

¹Shandong Provincial Key Laboratory of Optical Astronomy and Solar-Terrestrial Environment, School of Space Science and Technology, Shandong University, Weihai, China. ²Department of Endocrinology, Qilu Hospital of Shandong University (Qingdao), Qingdao, China. ³Department of Social Work, Shandong University, Weihai, China. ⁴School of Mathematics and Statistics, Shandong University, Weihai, China. ⁵Department of Gastrointestinal Surgery, Weihai Municipal Hospital, Cheeloo College of Medicine, Shandong University, Weihai, China. ⁶College of Science, Tibet University, Lhasa, China. ⁷Key Laboratory of Cosmic Rays, Tibet University, Ministry of Education, Lhasa, China. ⁸School of Ecology and Environment, Tibet University, Lhasa, China. ⁹School of Space and Earth Sciences, Beihang University, Beijing, China. ¹⁰Department of Oncology, McMaster University, Hamilton, Canada. ¹¹Department of Pulmonary and Critical Care Medicine, Qilu Hospital, Shandong University, Jinan, China. ¹²School of Earth and Space Sciences, Peking University, Beijing, China. ¹³These authors contributed equally: Pengzhi He, Chen Li. ✉e-mail: 18660377179@163.com; sqq@sdu.edu.cn

on the cardiovascular system is thought-provoking and demands more precise substantiation. Since the 20th century, pioneering efforts have advanced fields such as “heliobiology”, “chronoastronomy”, and “clinical cosmobiology”, exploring the influence of solar and lunar movements on human life systems and biological rhythms^{4–8}. Extensive research indicates that cardiovascular diseases such as myocardial infarction and cardiac death, as well as heart rate variability, exhibit significant statistical correlations with solar activity, GMA, and cosmic rays^{9–13}. Additionally, brain disorders like stroke are more likely to occur during periods of solar maximum and geomagnetic storms^{14–16}. Analyses of the temporal rhythms in biophysiological phenomena revealed that certain space weather parameters and BP fluctuations have similar periodicities. For instance, circadian rhythms have been found to exhibit correlations with short-term space weather disturbances^{17–20}, while long-term fluctuations in hypertension and associated mortality seem to be correlated with the approximately 11-year solar cycle^{21,22}. It has been well-documented that systolic BP and diastolic BP tend to increase during periods of elevated GMA, with this effect being particularly pronounced during geomagnetic storms^{23–26}. Overall, the intensity variations in GMA could lead to functional changes in the cardiovascular system²⁷, and the mortality associated with hypertension illness are highly correlated with various heliophysical parameters^{16,22}.

Due to the significant geomagnetic field variation, the cardiovascular system’s response to GMA at high magnetic latitudes has attracted major attention. The intensity of GMA is influenced by various current systems. In polar regions, these currents are mainly concentrated around 100 kilometers above the Earth’s surface, while in mid- and low-latitude areas, they are located several thousand to tens of thousands of kilometers from the surface^{28,29}. The sun continuously emits streams of charged particles, forming the solar wind, which consistently impacts the Earth, driving current systems in the magnetosphere to trigger GMA. During GMA, the polar current systems vary rapidly, and the current

density is enhanced, leading to strong and rapidly changing localized electromagnetic induction effects on Earth’s surface. At mid- and low latitudes, the amplitude of the magnetic field variation is smaller and varies more smoothly than that at high-latitude^{30,31}. The drastically changed electromagnetic induction in high magnetic latitudes leads to a conceivable impact on the cardiovascular system, while the impactation at lower latitudes attracts much less attention. Compared to the complex rapid variations of the polar magnetic field, the relatively moderate magnetic perturbation in the middle and low magnetic latitudes provides a more straightforward situation for assessing the effect of GMA on the cardiovascular system. In this study, we collated the BP measurement data from Qingdao and Weihai in China, two cities at mid-magnetic latitudes with uncomplicated geomagnetic environments and good air quality, and assessed the correlation between BP and GMA. Subsequently, we conducted a comparative analysis between environmental factors (air temperature and PM2.5) and GMA, revealing that BP and GMA exhibit similar annual bimodal patterns and multiple periodicities (3-month, 6-month, 12-month) that cannot be explained by air temperature and PM2.5. In general, our statistical study links the fluctuations between GMA and BP, revealing a correlation between human BP and the subtle yet influential signals from the geomagnetic field. These findings hold promise for the development of innovative strategies aimed at mitigating BP elevation.

Methods

Blood pressure data

The BP measurements were obtained from the Qilu Hospital of Shandong University (Qingdao) and the Weihai Municipal Hospital in China. The data were directly output by the hospitals and no sampling was required. Figure 1 shows the number of BP measurements and of individuals with hypertension from January 2015 to December 2020, subdivided according to gender. The total sample size is 554,319, of which 298,365 are males and

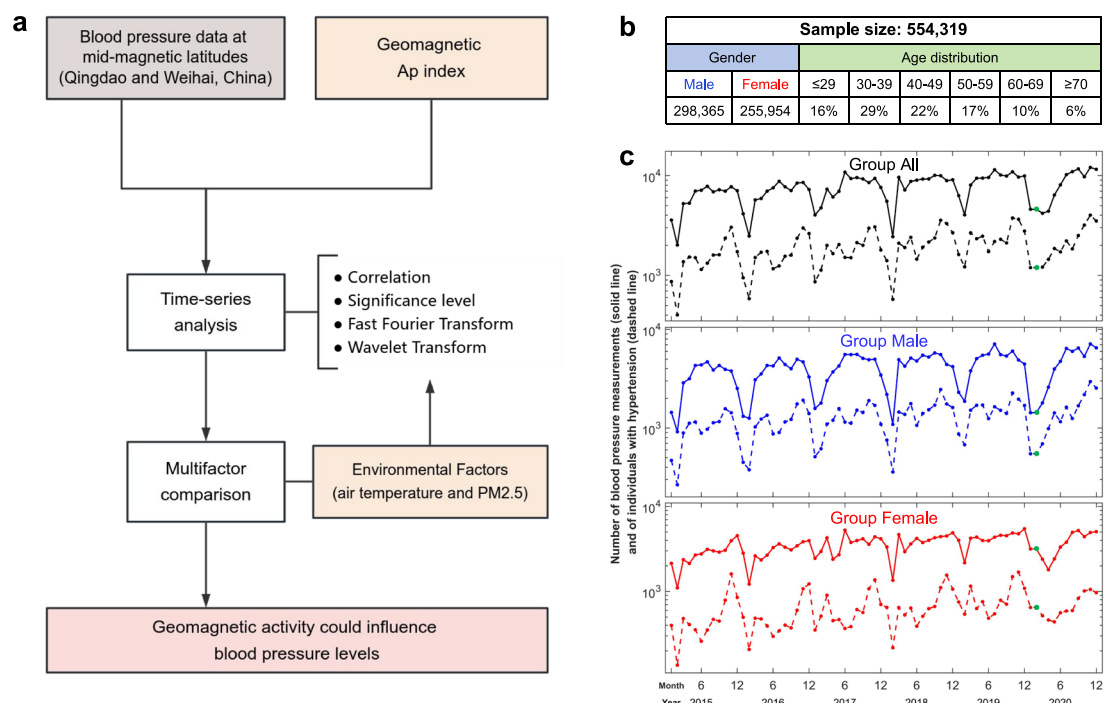


Fig. 1 | Study design and samples. a Study design. **b, c** Sample Characteristics. **b** The sample size and the distribution of gender and age. **c** Overview of the blood pressure (BP) measurements and hypertension in samples. The monthly number of BP measurements (solid line) and hypertension (dashed line) in three groups from January 2015 to December 2020. Group All, black lines, as a reference containing

both males and females; Group Male, blue lines; Group Female, red lines. These green points represent the continuation of the January 2020 data to February 2020, where original data was missing, using the Last Observation Carried Forward (LOCF) method.

255,954 are females. The total number of individuals with hypertension is 141,810, of which 93,549 are males and 48,261 are females. The prevalence of hypertension in the total sample is 25.58%, 31.35% for males, and 18.86% for females. The age range of the participants is broad, spanning from 11 to 103 years. The majority of the sample population (78%) falls within the 30–69 age group. These populations mainly lived in and around the cities of Qingdao and Weihai. Hypertension was defined as a systolic BP ≥ 140 mmHg and/or a diastolic BP ≥ 90 mmHg. BP is measured using OMRON Blood Pressure Monitors made in Japan, and rest is required before measurement to ensure accurate readings. All BP data are freely accessible and available in the Supplementary Data.

This retrospective study focuses solely on the statistical data of physical examinations and does not reveal personal information about any participants. It was approved by the Ethics Committee of Qilu Hospital of Shandong University (Qingdao) and Ethics Committee of Weihai Municipal Hospital in China, which confirmed that informed consent was not required and ensured full compliance with ethical guidelines and regulations.

The number of people taking BP measurements reaches its lowest level around February each year (Fig. 1c), coinciding with the Chinese New Year period when hospitals only conduct physical exams for employees. However, from March to January of the following year, the number of tests remains relatively stable. Furthermore, there were no BP measurements in hospitals due to Covid-19 in February 2020, so we duplicated and used the data from January 2020 to maximize data integrity based on the Last Observation Carried Forward (LOCF) method^{32,33}. Incomplete data may lead to errors in periodicity analysis. In addition, various methods for handling missing data including linear or polynomial interpolation were considered. To maintain data consistency and reduce potential variability that may arise from more complex interpolation methods, we chose the relatively conservative but robust LOCF method. The GMA, air temperature, and PM2.5 for February 2020 have been handled in the same method. All of the data were averaged on a monthly basis, hence each data point corresponds to a single month, which ensures a balance between data resolution and manageability, allowing us to capture seasonal and long-term trends without being overwhelmed by short-term noise.

Geomagnetic activity, air temperature and PM2.5 data

To assess GMA, we obtained the daily Ap index from the GFZ German Research Centre for Geosciences³⁴ (<https://www.gfz-potsdam.de/en/section/geomagnetism/data-products-services>). The Ap index serves as a global indicator of the intensity of full-day geomagnetic disturbances. This index was chosen for its comprehensive and continuous data coverage, making it suitable for long-term analysis in our study. The air temperature and PM2.5 data were obtained from reliable sources, including the China Weather Network (<https://www.tianqi.com/>), the Ministry of Ecology and Environment of the People's Republic of China, and the Weihai Municipal Ecological Environment Bureau (<https://www.mee.gov.cn/hjzl/dqhj/> and <https://sthjj.weihai.gov.cn/col/col45185/index.html>). These data, measured by many meteorological and air quality monitoring stations distributed across various districts and counties in each city, provide comprehensive and accurate information regarding the air temperature and PM2.5. All the data are freely accessible and available in the Supplementary Data. Consistent with the BP data processing approach, the geomagnetic, air temperature and PM2.5 data are also processed as monthly averages. The air temperature and PM2.5 used are average data for the city where the hospital is located. For PM2.5, the existing long-term records only have monthly average data, since higher cadence data is not available.

Analytical methods

Firstly, the Ap index was detrended using the moving average method^{35,36}. Studies have shown that GMA influenced by solar activity exhibits periodic characteristics of 4–6 years and 11 years³⁷. To remove the long-term trend and keep the short-period variation as analyzed below, we set the smoothing window to 36 months (i.e., 36 points). By detrending the data, it becomes easier to identify short-term changes and cyclic patterns that may be

obscured by long-term trends. This is particularly useful in time series analysis or when comparing data from multiple sources³⁸.

Subsequently, the data were tested for normality to determine whether certain statistical methods could be appropriately applied, such as Pearson or Spearman correlation³⁹. Cross-correlation and Spearman correlation methods were employed to examine the statistically averaged lag time and correlation coefficients between the monthly mean BP and Ap index⁴⁰. Cross-correlation is a statistical measure that quantifies the similarity between two time series. It examines the correspondence between patterns, variations, or changes in the data, allowing for the analysis of relationships and time delays⁴¹. Spearman correlation assesses the monotonic relationship between two variables, measuring the strength of correlation of their levels. Unlike Pearson correlation, it is not limited to linear relationships⁴². The significance levels were set at 0.05, 0.01, and 0.001, indicating the threshold for statistical significance. These significance levels are crucial for hypothesis testing. In null hypothesis testing, the null hypothesis typically posits that there is no statistically significant relationship between the variables being examined. The significance levels indicate the probability threshold below which the null hypothesis is rejected⁴³. Therefore, the null hypothesis was tested by comparing the calculated correlation coefficient (r) to these threshold values. If the p -value was less than the chosen significance level, it indicated a statistically significant relationship between the variables.

Additionally, the periodicities of these variables were determined using the Fast Fourier Transform (FFT), Continuous Wavelet transform (CWT) and Cross-Wavelet Transform (XWT) to understand the key patterns of temporal fluctuations. FFT is an efficient algorithm for computing Discrete Fourier Transform. It transforms a time-domain signal into its frequency-domain representation, enabling the analysis of periodicity, frequencies, and amplitude components⁴⁴. CWT and XWT are powerful tools for time-frequency analysis. CWT is commonly used for the detection of individual time series, while XWT is used to detect the coherence and phase relationships between two time series, thereby identifying common patterns and shared oscillation behaviors⁴⁵. All analytical methods were conducted using MATLAB R2020a.

Reporting summary

Further information on research design is available in the Nature Portfolio Reporting Summary linked to this article.

Results

Annual bimodal pattern and correlation analysis of BP and GMA

To illustrate the time-series characteristics of the BP and GMA, where GMA is denoted by the internationally recognized Ap index describing shifts in the geomagnetic field, we highlighted their bimodal distributions along with the time differences corresponding to their peaks (Fig. 2). The monthly mean Ap index and BP are shown to provide an overview of their fluctuations within each year (Fig. 2a–c). The peaks occurring in spring and autumn are clearly highlighted by the solid black line, which represents the 6-year average values. Furthermore, the peaks in BP exhibit apparent time delays with respect to the peaks in Ap. The original and detrended Ap index (Detrended-Ap), along with systolic BP and diastolic BP for various groups (indicated by the black line for all samples, blue line for male samples, and red line for female samples), are shown to indicate their long-term fluctuations (Fig. 2d–f). Trend analysis of the six-year data showed an overall decrease in the Ap index, while BP remained stable with no statistically significant upward or downward trends.

To aid in identifying the peaks and corresponding months, we positioned several vertical dashed lines (Fig. 2d–f). The systolic BP exhibits two peaks annually, observed during the months of April–May and October–November, accompanied by a trough in close proximity to June. These peaks are more pronounced in Group Female, with the first peak being substantially weaker than the second. Notably, additional peaks can be observed in the male data, such as in May 2017 and January 2018. The data of Group All, indicated by the center black line, are used as reference values (Fig. 2e). The distribution of the bars in Fig. 2e illustrate the difference

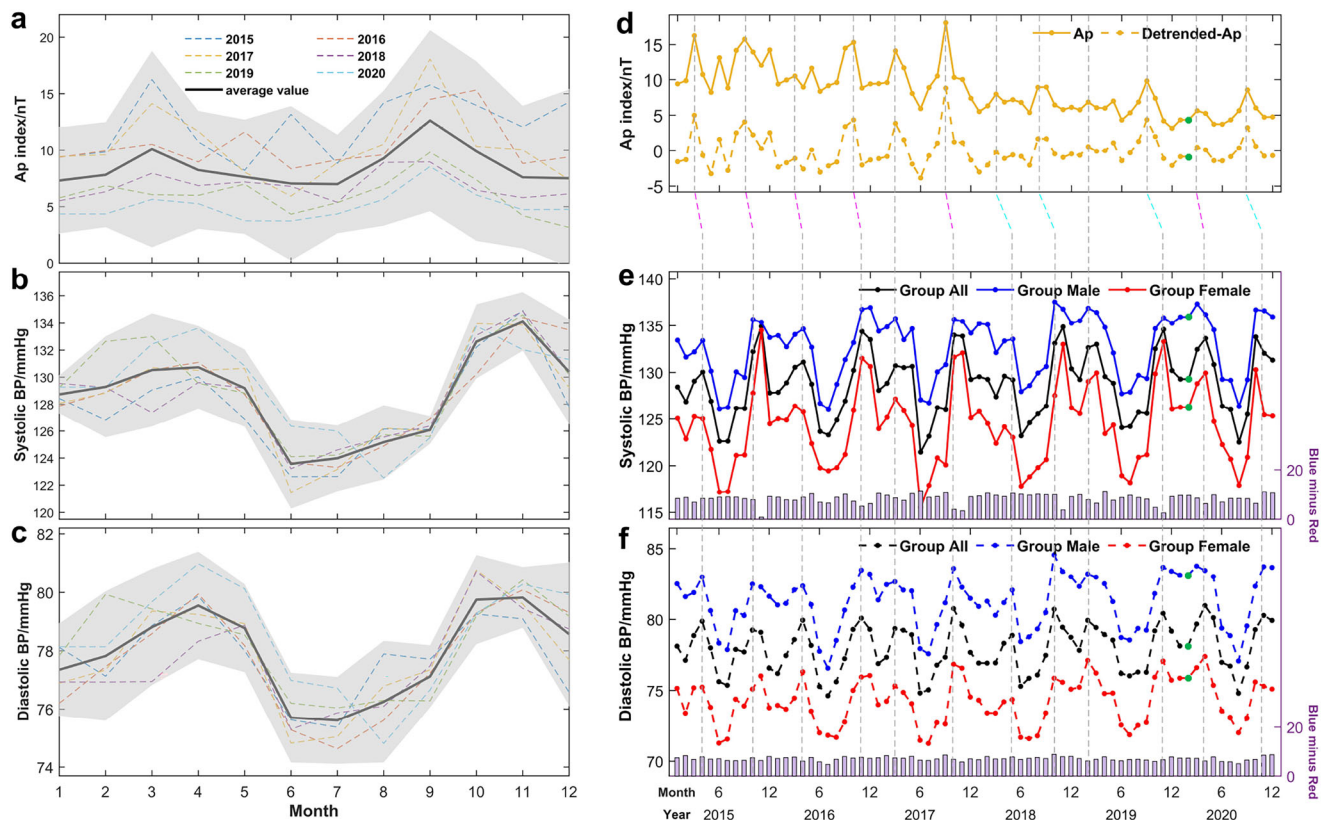


Fig. 2 | Bimodal distribution of Ap index and blood pressure. a–c Monthly fluctuations of Ap index, systolic blood pressure (BP), and diastolic BP. Dashed lines of different colors represent different years (2015–2020), while the thick black solid lines represent the mean of the 6-year data. The upper and lower boundaries of the shaded areas are the mean plus and minus twice the standard deviation, respectively. d The monthly mean Ap index (solid line) and Detrended-Ap (dashed line) from January 2015 to December 2020. e, f The monthly mean systolic BP (solid line) and diastolic BP (dashed line) in three groups from January 2015 to December 2020.

Black for Group All; Blue for Group Male; Red for Group Female. The sample size of BP measurements is 554,319, with 298,365 for Group Male and 255,954 for Group Female. The purple bar chart represents the data of blue minus red. The dashed lines running through (d–f) highlighted the peaks at the corresponding time. The pink and blue turning lines indicate that the peak time of BP is 1 month and 2 months later than Ap, respectively. These green points represent the continuation of the January 2020 data to February 2020, where original data was missing, using the Last Observation Carried Forward (LOCF) method.

between the systolic BP for males and females, indicating that the difference is smallest in October or November of each year compared to the other months. The diastolic BP is presented in Fig. 2f, with peaks and troughs occurring at the same time as the systolic BP. In Group Female, the difference between the two annual peaks in diastolic BP is smaller compared to systolic BP. Additionally, the first peak in diastolic BP per year is notably smaller than the second peak. The variability of diastolic BP in Group All is less than that of systolic BP, with an amplitude difference calculated according to variance is approximately 10 mmHg. Overall, diastolic BP consistently appears higher in Group Male than in Group Female.

A downward trend in the Ap index can be observed during the analysis time (Fig. 2d). The Ap index also exhibits two peaks each year, occurring in March–April and September–October, which is 1–2 months ahead of the BP. Time differences of 1-month or 2-month were estimated between BP and Ap index based on the cross-correlation method⁴¹. The gray dashed lines spanning panels d to f indicate a zero time lag between the Ap index and BP, observed in the first half of 2017 and 2019. The pink turning lines below panel d indicate that the peak in BP is 1 month later than the peak in Ap index, primarily observed in 2017 and before. Similarly, the blue turning lines below panel d indicate that the peak in BP is 2 months later than the Ap index peak, primarily observed in 2018 and beyond. In general, the relationship between the peak time in BP and the Ap index during the period of 2015–2017 exhibited a 1-month lag. However, from 2018 to 2020, there was an observed increase in the statistically averaged lag time, with BP showing a 2-month delay in its response.

The analysis indicates a temporal difference of 1-month or 2-month, which occurs in the first and second three-year periods, respectively. To account for this, the calculation process was separated into two temporal phase differences and three different time series (represented as I, II, III, i.e. 2015.1–2020.12, 2015.1–2017.12, 2018.1–2020.12). The data of BP and Ap index (or Detrended-Ap) did not follow a fully normal distribution according to the Jarque-Bera test⁴⁶, so Spearman correlation was chosen to be calculated between the monthly mean BP and Detrended-Ap separately for different groups and periods. The Spearman correlation coefficient (r_s) results are shown in Tables 1 and 2, and graphed results are provided in Supplementary Figs. 1 and 2. The content in parentheses indicated Detrended-Ap were either 1-month or 2-month ahead of the BP. We found a statistically significant correlation between systolic BP for Group All and Detrended-Ap at a 1-month lead in time series I ($r_s=0.409$, $p=0.0004$). The correlation remained significant after distinguishing gender (Group Male: $r_s=0.347$, $p=0.0029$; Group Female: $r_s=0.365$, $p=0.0016$) (Table 1). When the correlation reached its maximum, the time difference was clearly 1 month during time series II and 2 months during time series III. Table 2 shows the r_s results between diastolic BP and Detrended-Ap for the different time series. During the 6-year study period, Detrended-Ap is significantly 1-month ahead of diastolic BP for Group All ($r_s=0.421$, $p=0.0002$). The correlation in the time series II and III follows the same pattern as that of systolic BP (Table 2). Overall, the Ap index, which is used to characterize the level of GMA, shows a significant positive correlation with systolic BP and diastolic BP. Furthermore, except for the diastolic BP in Group Male in time

Table. 1 | Correlation analysis: Spearman correlation coefficient and significance level (ρ) between systolic blood pressure (BP) and Detrended-Ap

	Time series		
	I. 2015.1–2020.12	II. 2015.1–2017.12	III. 2018.1–2020.12
	Group All		
Detrended-Ap (lead 1)	0.409 ($\rho = 0.0004^{***}$)	0.516 ($\rho = 0.0015^{**}$)	0.351 ($\rho = 0.0358^*$)
Detrended-Ap (lead 2)	0.407 ($\rho = 0.0004^{***}$)	0.434 ($\rho = 0.0087^{**}$)	0.416 ($\rho = 0.0116^*$)
	Group Male		
Detrended-Ap (lead 1)	0.267 ($\rho = 0.0239^*$)	0.470 ($\rho = 0.0042^{**}$)	0.174 ($\rho = 0.3116$)
Detrended-Ap (lead 2)	0.347 ($\rho = 0.0029^{**}$)	0.467 ($\rho = 0.0045^{**}$)	0.282 ($\rho = 0.0953$)
	Group Female		
Detrended-Ap (lead 1)	0.365 ($\rho = 0.0016^{**}$)	0.513 ($\rho = 0.0016^{**}$)	0.267 ($\rho = 0.1152$)
Detrended-Ap (lead 2)	0.363 ($\rho = 0.0017^{**}$)	0.391 ($\rho = 0.0191^*$)	0.337 ($\rho = 0.0447^*$)

The systolic BP data is divided into three time series: I (2015.1–2020.12), II (2015.1–2017.12), and III (2018.1–2020.12). Detrended-Ap values from one or two months prior to systolic BP are used in the calculation process, indicated by “lead 1” and “lead 2” in parentheses, respectively. The significance levels are denoted as $^*p < 0.05$, $^{**}p < 0.01$, and $^{***}p < 0.001$. Additionally, the sample group was stratified by gender.

Table. 2 | Correlation analysis: Spearman correlation coefficient and significance level (ρ) between diastolic blood pressure (BP) and Detrended-Ap

	Time series		
	I. 2015.1–2020.12	II. 2015.1–2017.12	III. 2018.1–2020.12
	Group All		
Detrended-Ap (lead 1)	0.421 ($\rho = 0.0002^{***}$)	0.521 ($\rho = 0.0013^{**}$)	0.391 ($\rho = 0.0183^*$)
Detrended-Ap (lead 2)	0.341 ($\rho = 0.0034^{**}$)	0.335 ($\rho = 0.0465^*$)	0.422 ($\rho = 0.0100^{**}$)
	Group Male		
Detrended-Ap (lead 1)	0.304 ($\rho = 0.0095^{**}$)	0.510 ($\rho = 0.0017^{**}$)	0.195 ($\rho = 0.253$)
Detrended-Ap (lead 2)	0.310 ($\rho = 0.0080^{**}$)	0.314 ($\rho = 0.0624$)	0.359 ($\rho = 0.0316^*$)
	Group Female		
Detrended-Ap (lead 1)	0.358 ($\rho = 0.0020^{**}$)	0.517 ($\rho = 0.0015^{**}$)	0.259 ($\rho = 0.1265$)
Detrended-Ap (lead 2)	0.305 ($\rho = 0.0092^{**}$)	0.336 ($\rho = 0.0459^*$)	0.251 ($\rho = 0.1404$)

The diastolic BP data is divided into three time series: I (2015.1–2020.12), II (2015.1–2017.12), and III (2018.1–2020.12). Detrended-Ap values from one or two months prior to diastolic BP are used in the calculation process, indicated by “lead 1” and “lead 2” in parentheses, respectively. The significance levels are denoted as $^*p < 0.05$, $^{**}p < 0.01$, and $^{***}p < 0.001$. Additionally, the sample group was stratified by gender.

series III, most of the r_s results are slightly stronger in Group Female compared to Group Male.

Based on our analysis of the correlations and fluctuations, we conclude that there is a 1-month lag for BP from 2015 to 2017. However, a 2-month lag is the optimal response from 2018 to 2020. Notably, the r_s in time series II are generally higher than those in time series III, suggesting a stronger relationship between BP and Detrended-Ap. We speculate that the decrease of r_s in time series III can be attributed to the approach of the minimum phase in the 11 year solar cycle in GMA indicated by the Ap index consistently below 10nT (Fig. 2d).

Regarding gender-related differences, we found that 1–2 months after the Ap index reaches its second annual peak, the systolic BP for Group Female reaches its maximum in October–November of each year (Fig. 2e). Importantly, during this period, the difference in systolic BP between males and females is at its lowest, with an average difference of 3.89 mmHg. In all other months, the systolic BP for Group Male consistently surpasses that of Group Female, with an average difference of 8.95 mmHg. Additionally, the correlation analysis results between systolic BP and Detrended-Ap are slightly higher for Group Female compared to Group Male. However, the difference in diastolic BP depicted in the bar chart did not exhibit significant changes throughout the study period (Fig. 2f). In conclusion, our findings suggest that GMA has a more significant influence on women’s systolic BP, particularly after reaching the annual peaks in the Ap index.

Periodic characteristics of BP and GMA

To determine the periodic characteristics of BP and the Ap index, we applied Fast Fourier Transform (FFT)⁴⁴ to the Ap index and Detrended-Ap (Fig. 3a), as well as systolic BP and diastolic BP of different groups (Fig. 3b, c). We found that both Ap index and Detrended-Ap exhibit multiple periodicities over the 6-year data, with cycles at approximately 3, 6, and 12 months. The periodicity of the Ap index shows an increasing profile over the long term, indicating that there is a longer period character, but the sample is too limited to display meaningful results. Similarly, systolic BP and diastolic BP showed the same multi-cycle patterns as Ap index. For Group All, the amplitude of these cycles are roughly equal for systolic BP, while the 6-month cycle is more pronounced for diastolic BP. These findings indicate that BP and the Ap index share common 3-month, 6-month, and 12-month periodicities, although the strongest periodic signal is different.

The Cross-Wavelet Transform (XWT)⁴⁵ was employed to conduct a detailed time-frequency analysis, aiming to explore the precise correspondence and phase asynchrony between BP and Detrended-Ap. The XWT results displayed the dynamic periodic characteristics of the two sets of variables over time (Fig. 3d–i). The arrows in the time-frequency space pointing to the right or left indicate in-phase or anti-phase datasets, respectively⁴⁷. The numerous arrows pointing to the right within the thick black line indicate an in-phase behavior and a positive correlation between BP and Detrended-Ap. Some of these arrows also show an upward trend,

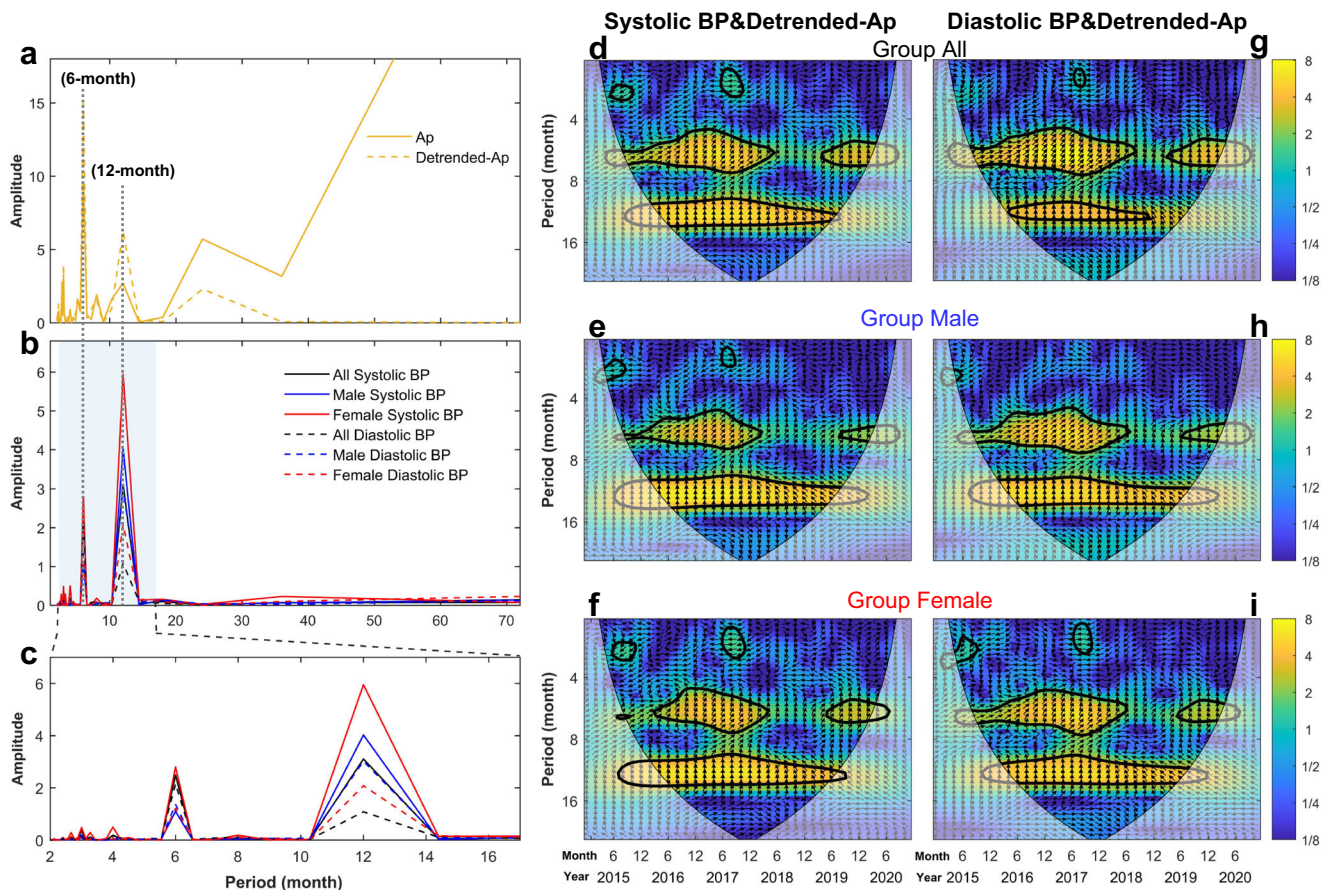


Fig. 3 | Periodic characteristics of Ap index and blood pressure. a–c Least squares spectra of Ap index and blood pressure (BP) based on the Fast Fourier Transform (FFT). **a** Ap index and Detrended-Ap. **b** Systolic BP and diastolic BP of three groups (Group All, Group Male, Group Female). **c** The shaded area in panel b is extended to highlight the detailed frequency characteristics of systolic BP and diastolic BP. **d–i** Cross-Wavelet Transform (XWT) of systolic BP and Detrended-Ap (**d–f**),

diastolic BP and Detrended-Ap (**g–i**). The color bar indicates the intensity of the period range, with yellow indicating the maximum value and blue indicating the minimum. The thick black contours mark the 95% confidence interval boundary that passes the red noise processes. The thin black line in the shaded area indicates the cone of influence (COI), which indicates the edge effect resulting from the finite-length time series. The arrows indicate the phase relationship between the variables.

suggesting that the phase of Detrended-Ap leads BP by a certain time interval, which aligns with the 1-month or 2-month time difference mentioned earlier. The XWT of systolic BP and Detrended-Ap revealed consistent cycles at 6-month and 12-month periods (Fig. 3d–f). After 2018, Group Female exhibits a slightly stronger 6-month cycle compared to Group Male, along with intermittent 3-month cycles observed in the second half of 2015 and 2017. The XWT of diastolic BP and Detrended-Ap, again showing the presence of 6-month and 12-month cycles (Fig. 3g–i). Notably, Group Female, particularly in relation to the brief 3-month cycle, exhibits a closer match with the cycle of the Ap index compared to Group Male. The strong 6-month cycle visible in all XWT images is truncated in early 2018, which we attribute to the reduction of the GMA level. Furthermore, we extracted the weekly mean data for the Ap index and BP, as shown in Supplementary Fig. 3. Based on the correspondence of the peaks, there is an observed statistically averaged lag time of approximately 3 to 10 weeks for BP. The results of the periodic analysis are shown in Supplementary Fig. 4. BP and Detrended-Ap index exhibit the same phase relationship, showing 12-week (3-month), 26-week (6-month), and 52-week (12-month) periodic characteristics.

Comparative analysis of the influence of environmental factors on BP

To establish the credibility and distinct contribution of GMA on BP, we conducted a comparative analysis with two other environmental factors (air temperature and PM2.5). The air temperature and PM2.5 in Qingdao and Weihai were significantly influenced by the seasons and exhibit a 12-month

periodicity (Fig. 4a–c). In terms of XWT (Fig. 4d–k), it is clear that air temperature and BP only share a 12-month periodicity, PM2.5 and BP share consistent 12-month and 6-month periodicities. However, the 6-month periodicity of PM2.5 is significantly weaker compared to the Ap index. Most importantly, PM2.5 does not exhibit a 3-month periodicity. This supports our view that GMA fluctuations exhibit spectral characteristics that correlate well with the BP fluctuation spectrum.

For the correlation analysis, previous studies indicate that BP responds to changes in air temperature and PM2.5 within days or hours^{48,49}. Using monthly average data, our cross-correlation analysis also showed no time lag, so it was not necessary to account for lag when calculating r_s . The correlations with systolic BP were generally strong (Qingdao air temperature: $r_s = -0.365$, $p = 0.0016$; Weihai air temperature: $r_s = -0.650$, $p = 0.0001$; Qingdao PM2.5: $r_s = 0.266$, $p = 0.0240$; Weihai PM2.5: $r_s = 0.319$, $p = 0.0063$), while the correlations with diastolic BP were slightly weaker (Qingdao air temperature: $r_s = -0.253$, $p = 0.0317$; Weihai air temperature: $r_s = -0.493$, $p = 0.0001$; Qingdao PM2.5: $r_s = 0.119$, $p = 0.3195$; Weihai PM2.5: $r_s = 0.286$, $p = 0.0148$). To summarize, compared to Detrended-Ap, air temperature exhibited a stronger correlation with BP, while PM2.5 showed a weaker correlation.

Discussion

This study confirms an observable relationship between BP in mid-magnetic latitude populations and solar-terrestrial system patterns, based on long-term medical statistics. Our findings provide evidence linking fluctuations between GMA and BP, indicating that elevated GMA levels

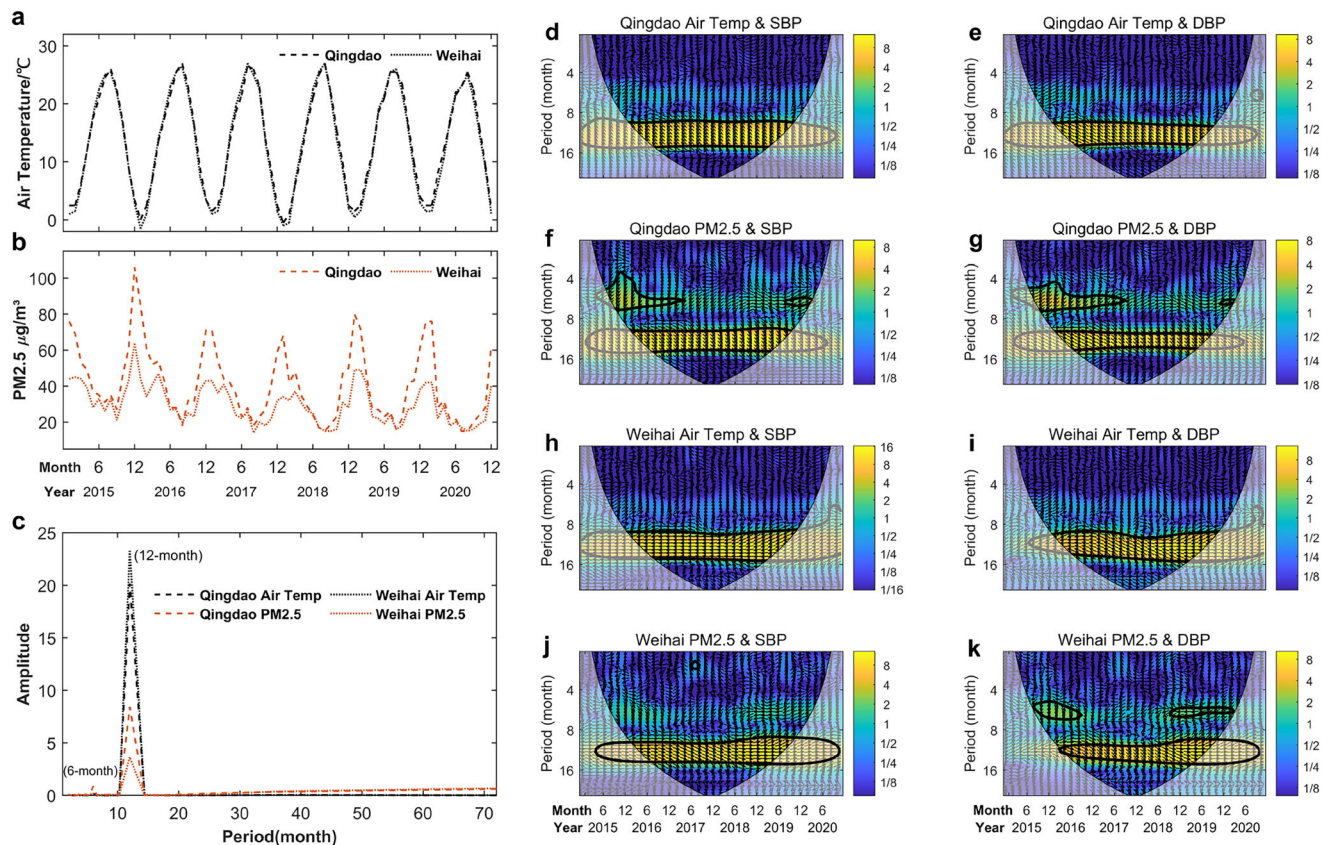


Fig. 4 | Air temperature and PM2.5. **a, b** The monthly mean air temperature and PM2.5 in Qingdao and Weihai from January 2015 to December 2020. **c** Least squares spectra of air temperature and PM2.5 based on the Fast Fourier Transform (FFT). **d–k** Cross-Wavelet Transform (XWT) of blood pressure with air temperature and PM2.5 in Qingdao (**d–g**) and Weihai (**h–k**). The color bar indicates the intensity of

the period range, with yellow indicating the maximum and blue indicating the minimum. The thick black contours mark the 95% confidence interval boundary that passes the red noise processes. The thin black line in the shaded area indicates the cone of influence (COI), which indicates the edge effect resulting from the finite-length time series. The arrows indicate the phase relationship between the variables.

may pose potential risks to individuals with hypertension. This could inform healthcare policymakers to recognize the clinical significance of the geomagnetic environment.

Considering the hospital's work arrangement, which includes a balance between spontaneous and group appointments for medical check-ups, and the scheduling of physical exams three months in advance, we have minimized the possibility of including excessive BP data due to sudden hypertension. Furthermore, by examining the solid and dashed lines in Fig. 1c, it becomes evident that the number of individuals with hypertension does not always directly increase or decrease in conjunction with the number of BP measurements. This situation occurs frequently, such as in April–May 2015, when an increase in the number of BP measurements was accompanied by a decrease in the number of individuals with hypertension. This suggests that the data follow unknown patterns over time, and this conclusion remains consistent when analyzing the data separately by gender. That is to say, the monthly mean BP data fluctuates randomly and is independent of the number of BP measurements. However, the BP measurements does not include specific records on the use of BP medications. Medical history and medication records are only available for outpatient and inpatient data. BP measurements from health check-up centers cannot be matched with these information.

We use the Ap index to define three intensity levels for the GMA, with Ap ranging from 0–7nT for quiet, 8–15nT for unsettled, and 16–29nT for active periods⁵⁰. The Ap index ranged from 3 to 18 nT over the entire study period (Fig. 2d). In the first three years, it averaged 11.12 nT, mostly in the unsettled category with occasional peaks in the active category. In the last three years, it averaged 6.08 nT, mainly in the quiet category. According to the time-series data shown in Fig. 2d–f, BP did not exhibit an overall decrease

or increase over the 6-year study period. Instead, it remained relatively stable. This indicates that inter-annual changes in the intensity of GMA do neither increase nor decrease overall BP levels in the population over the long term. However, in terms of annual changes, the effect on BP varies depending on the intensity of GMA. In unsettled times, we observed a statistically averaged lag time of 1 month, while during quiet times, the statistically averaged lag time was mainly 2 months. This indicates that the time delay between GMA and BP changes differs based on GMA intensity. Despite exceptions like the first peak of 2019, there is no significant time lag, as shown in Fig. 2d. This may be due to other factors influencing BP becoming more significant in years with lower GMA, causing the interpretation of time lag to be less clear. However, individual data points deviating from the average can be smoothed out across multiple years of statistical analysis. Similarly, some studies have investigated the effects of strong GMA on BP, such as during geomagnetic storm periods ($A_p > 30$ nT). They have reported rapid changes in BP within a few days and an increase in cardiovascular-related illnesses or hospital admissions^{23,24}. These previous findings do not contradict the results reached in this paper—rather we come to the analogous and more general conclusion that the higher the GMA level, the shorter the statistically averaged lag time of BP fluctuations.

The fluctuations in population BP in response to Ap index have been elucidated, moreover, some slight differences in BP trends have emerged between males and females. For the second peak of systolic BP each year, Group Female exhibits a rapid rise and decline. In contrast, Group Male sustains elevated levels for 1–2 months after the peak, with a significantly smaller increase and decrease compared to Group Female (Fig. 2e). This could be because women, especially in younger age groups, have a higher concentration of vasodilatory substances and anti-inflammatory pathways

than male and postmenopausal female. Furthermore, the female is more likely to develop vasodilation, enabling a quicker return to normal BP⁵¹. The World Health Organization (WHO) reports that the age of natural menopause in women worldwide is generally between 45 and 55 years. A study investigating over 1,000 menopausal women in and around the Qingdao urban area, found the average age of menopause onset to be 49.44 ± 3.27 years old⁵². Similarly, another study in Weihai reported an average menopausal age of 49.09 ± 4.12 years old⁵³. In the sample of this study, women under the age of 50 make up approximately 68% of all female participants. In addition, compared to Group Male, Group Female exhibited slightly stronger correlations between BP and Detrended-Ap, as well as more consistent cycles. These findings provide further statistically significant evidence of correlations that are consistent with previous studies that women may be more susceptible to the effects of GMA on BP^{18,54}.

Some studies have investigated the relationship between BP from different latitude regions and GMA, such as Canada²², the United States⁵⁵, and Mexico²¹, but there is a lack of comparative studies on the influence of latitude differences in BP response. We have investigated do we see any signatures of influence of latitude on the relationship between GMA and BP in our dataset. Both cities exhibit consistent fluctuation patterns, with peaks occurring in April-May and October-November (Supplementary Fig. 5). Supplementary Table 1 and 2 show the correlation between Detrended-Ap and systolic BP, as well as diastolic BP, respectively. The r_s results of systolic BP in Qingdao are slightly higher, however, there is no significant latitude difference effect on diastolic BP. Qingdao is located between latitudes $35^\circ 35' N$ and $37^\circ 09' N$, while Weihai is located between $36^\circ 41' N$ and $37^\circ 35' N$. Due to the very small differences in latitude, drawing statistically significant conclusions is challenging and requires more data from cities at different latitudes.

This study used air temperature and PM2.5 as independent environmental factors. Air temperature is intrinsically intertwined with atmospheric pressure and humidity⁵⁶, thereby effectively encompassing most environmental factors known to influence human sensory experiences. Blood vessels regulate body temperature through constriction and dilation. Blood vessels constrict when the air temperature decreases, leading to a rise in BP; and dilate when the weather is hot, leading to a fall in BP⁴⁹. Several studies have indicated that exposure to PM2.5 has detrimental effects on BP^{48,57}. Consistent with prior studies, our research reaffirmed the significant correlation between BP and these environmental factors (both air temperature and PM2.5). Although the effects of air temperature and PM2.5 on BP are important and cannot be ignored, they did not exhibit the annual bimodal patterns and multiple periodicities. Similarly, research showed that air pressure and humidity also exhibit primarily annual fluctuations^{58,59}, with no multiple cycles consistent with BP. Remarkably, only GMA showed a stronger connection with BP in terms of these periodic characteristics.

Based on existing statistical data, it is challenging to ascertain which gender is more sensitive to temperature or PM2.5 levels. As shown in Supplementary Figs. 6 and 7, the correlation between BP and air temperature follows a more nonlinear pattern, while the correlation between BP and PM2.5 is linear. For both air temperature and PM2.5, females in Weihai showed higher correlations, whereas males in Qingdao had stronger correlations. Therefore, we are currently unable to draw conclusions about gender differences in the effects of air temperature and PM2.5 on BP, and future research requires data from more cities.

The occurrence of two peaks each year and the 6-month periodicity of GMA can be attributed to the occurrence of strong geomagnetic storm events that are triggered by the Interplanetary Magnetic Field (IMF). These events have a higher likelihood of occurring around the annual vernal equinox (autumnal equinox) when the IMF is aligned toward (away from) the sun. This mechanism is commonly explained by both the Russell-McPherron effect and the equinoctial effect, which are widely accepted in the scientific community^{60–62}. The influence of GMA on human health is believed to be mediated through direct or indirect pathways⁶³, with one potential indirect method being through primary effects in the brain that

cascade downstream via the vagus nerve. Future research is required to collect the patient data where vagus nerves were removed/severed surgically (or inhibited pharmaceutically), with the aim to explore the role of the vagus nerve in mediating the effects of GMA on BP. Additionally, previous research has found strong correlations between Schumann resonance signals and GMA indices, with both exhibiting common periodicities such as 27 days, 3-month, and half a year cycles^{64,65}. One possible mechanism explaining the effect of GMA on BP involves the modulation of ultra-low frequency waves, specifically Schumann resonances and their harmonics, which occur within the Earth's magnetosphere and ionospheric cavities. The fundamental frequency of Schumann resonances is approximately 7.8 Hz, with harmonics around 14.1, 20.3, 26.4, and 32.5 Hz⁶⁶. These fluctuations may interfere with human brain waves such as alpha (8–12 Hz), beta (12–30 Hz), and gamma (30–100 Hz), which have been demonstrated by monitoring subjects' electroencephalograms (EEGs) in some studies^{11,67–69}. The brain may then send instructions to secrete hormones to cause changes in BP within the body. Several studies have indicated that the density of neurons containing vasopressin, a hormone involved in regulating BP, peaks in May and November each year^{70,71}, which roughly corresponds to the peak times of BP mentioned in this paper. During periods of high neuron density and increased vasopressin levels, the kidneys reabsorb more water, leading to elevated BP. Therefore, it is plausible to speculate that vasopressin acts as an intermediate factor contributing to the increase in BP induced by elevated GMA.

Our analysis supplement previous research, indicating that GMA has an in-phase effect on BP and shows consistency across multiple cycles. Higher intensity of GMA leads to faster changes in BP. There was a statistically averaged lag time of approximately 1–2 months, from GMA change to BP change observed in this study. Given the randomness of the raw data and the rigor of the statistical analysis, we conclude that the findings are not coincidental. These findings expand our understanding of external factors contributing to BP fluctuations and enhance our comprehension of the intricate relationship between the geomagnetic environment and the human cardiovascular system. Future research may extend to a full solar cycle, as the degree and statistically averaged lag time of BP may differ as the range in GMA variations is increased. This study acknowledges its limitations, and it is important to note that establishing a causal relationship based solely on correlation statistics can be challenging. Correlation does not necessarily imply causation, and there may be other factors or variables that could lead to the observed correlations between BP and GMA.

Data availability

The data for this study are available in the supplementary data 1 and supplementary data 2. Supplementary Data 1 includes the number of blood pressure measurements and individuals with hypertension; systolic and diastolic blood pressure values, categorized by gender and hospital; and environmental parameters, including the geomagnetic activity Ap index, air temperature, and PM2.5 levels. It serves as the source data for Fig. 1, Fig. 2d–f, Fig. 3, Fig. 4, and Supplementary Figs. 1–7. Supplementary Data 2 includes systolic and diastolic blood pressure values with their mean and standard deviation, supporting Fig. 2a–c. Additionally, the Ap index data are publicly available at <https://www.gfz-potsdam.de/en/section/geomagnetism/data-products-services>. The air temperature data are available at <https://www.tianqi.com/>. The PM2.5 data are available at <https://www.mee.gov.cn/hjzl/dqhj/> and <https://sthjj.weihai.gov.cn/col/col45185/index.html>. All datasets are freely accessible.

Code availability

The code used for data analysis and plotting is available in a Zenodo Repository⁷².

Received: 12 November 2023; Accepted: 25 March 2025;

Published online: 28 April 2025

References

- Hahad, O., Daiber, A. & Muenzel, T. Reduced aircraft noise pollution during COVID-19 lockdown is beneficial to public cardiovascular health: a perspective on the reduction of transportation-associated pollution. *Hypertension* **79**, 335–337 (2022).
- Huang, K. et al. Long-term exposure to fine particulate matter and hypertension incidence in China: the China-PAR cohort study. *Hypertension* **73**, 1195–1201 (2019).
- Modesti, P. A. et al. Weather-related changes in 24-hour blood pressure profile—effects of age and implications for hypertension management. *Hypertension* **47**, 155–161 (2006).
- Breus, T. K., Vladimirovskii, B. M. & Zelenyi, L. M. Unfinished debates on the 120th anniversary of the birthday of A.L. Chizhevsky. *Her. Russian Acad. Sci.* **87**, 535–542 (2017).
- Gumarova, L., Cornelissen, G., Hillman, D. & Halberg, F. Geographically selective assortment of cycles in pandemics: meta-analysis of data collected by Chizhevsky. *Epidemiol. Infect.* **141**, 2173–2184 (2013).
- Halberg, F. et al. Chronoastrobiology: proposal, nine conferences, heliogeomagnetics, transyears, near-weeks, near-decades, phylogenetic and ontogenetic memories. *Biomed. Pharmacother.* **58**, S150–S187 (2004).
- Otsuka, K. et al. Chronomics for chronoastrobiology with immediate spin-offs for life quality and longevity. *Biomedicine Pharmacother.* **57**, 1S–18S (2003).
- Stoupel, E., Petrauskienė, J., Kaledienė, R., Abramson, E. & Sulkes, J. Clinical cosmobiology—the Lithuanian study 1990–1992. *Int. J. Biometeorol.* **38**, 204–208 (1995).
- Alabdulgader, A. et al. Long-term study of heart rate variability responses to changes in the solar and geomagnetic environment. *Sci. Rep.* **8** (2018).
- Knox, E. G., Armstrong, E., Lancashire, R., Wall, M. & Haynes, R. Heart attacks and geomagnetic-activity. *Nature* **281**, 564–565 (1979).
- McCraty, R. et al. Synchronization of human autonomic nervous system rhythms with geomagnetic activity in human subjects. *Int. J. Environ. Res. Public Health* **14** (2017).
- Samsonov, S. N., Kleimenova, N. G., Kozyreva, O. V. & Petrova, P. G. The effect of space weather on human heart diseases in subauroral latitudes. *Izvestiya Atmos. Oceanic Phys.* **50**, 719–727 (2014).
- Vieira, C. L. Z. et al. Geomagnetic disturbances reduce heart rate variability in the normative aging study. *Sci. Total Environ.* **839** (2022).
- Feigin, V. L. et al. Geomagnetic storms can trigger stroke evidence from 6 large population-based studies in Europe and Australasia. *Stroke* **45**, 1639 (2014).
- Stoupel, E., Babayev, E. S., Abramson, E. & Sulkes, J. Days of “Zero” level geomagnetic activity accompanied by the high neutron activity and dynamics of some medical events—antipodes to geomagnetic storms. *Health* **05**, 855–861 (2013).
- Stoupel, E. et al. Twenty years study of solar, geomagnetic, cosmic ray activity links with monthly deaths number (n=850304). *J. Biomed. Sci. Eng.* **04**, 426–434 (2011).
- Azcarate, T. & Mendoza, B. Influence of geomagnetic activity and atmospheric pressure in hypertensive adults. *Int. J. Biometeorol.* **61**, 1585–1592 (2017).
- Azcarate, T., Mendoza, B., de la Pena, S. S. & Martinez, J. L. Temporal variation of the arterial pressure in healthy young people and its relation to geomagnetic activity in Mexico. *Adv. Space Res.* **50**, 1310–1315 (2012).
- Xiao, C. et al. Evidence for lunar tide effects in Earth’s plasmasphere. *Nat. Phys.* **19**, 486–491 (2023).
- Shi, Q. Q. et al. In *Dayside Magnetosphere Interactions* (eds Zong, Q., Escoubet, P., Sibeck, D., Le, G. & Zhang, H.) (CoLab, 2020).
- Azcarate, T., Mendoza, B. & Levi, J. R. Influence of geomagnetic activity and atmospheric pressure on human arterial pressure during the solar cycle 24. *Adv. Space Res.* **58**, 2116–2125 (2016).
- Caswell, J. M., Carniello, T. N. & Murugan, N. J. Annual incidence of mortality related to hypertensive disease in Canada and associations with heliophysical parameters. *Int. J. Biometeorol.* **60**, 9–20 (2016).
- Dimitrova, S., Stoilova, I. & Cholakov, I. Influence of local geomagnetic storms on arterial blood pressure. *Bioelectromagnetics* **25**, 408–414 (2004).
- Ghione, S., Mezzasalma, L., Del Seppia, C. & Papi, F. Do geomagnetic disturbances of solar origin affect arterial blood pressure? *J. Hum. Hypertension* **12**, 749–754 (1998).
- Khabarova, O. V. & Dimitrova, S. Some proves of integrated influence of geomagnetic activity and weather changes on human health. *Physics*. Preprint at <https://arxiv.org/abs/0810.0457> (2008).
- Wang, V. A. et al. Solar activity is associated with diastolic and systolic blood pressure in elderly adults. *J. Am. Heart Assoc.* **10** (2021).
- Dimitrova, S., Mustafa, F. R., Stoilova, I., Babayev, E. S. & Kazimov, E. A. Possible influence of solar extreme events and related geomagnetic disturbances on human cardio-vascular state: results of collaborative Bulgarian-Azerbaijani studies. *Adv. Space Res.* **43**, 641–648 (2009).
- Bonnevier, B., Bostrom, R. & Rostoker, G. A 3-Dimensional model current system for polar magnetic substorms. *J. Geophys. Res.* **75**, 107 (1970).
- Le, G., Russell, C. T. & Takahashi, K. Morphology of the ring current derived from magnetic field observations. *Annales Geophysicae* **22**, 1267–1295 (2004).
- Davis, T. N. & Sugiura, M. Auroral electrojet activity index ae and its universal time variations. *J. Geophys. Res.* **71**, 785 (1966).
- Rostoker, G. Polar magnetic substorms. *Rev. Geophys.* **10**, 157–211 (1972).
- Bourguignon, L. et al. Studying missingness in spinal cord injury data: challenges and impact of data imputation. *Bmc Med. Res. Methodol.* **24** (2024).
- Shao, J. & Zhong, B. Last observation carry-forward and last observation analysis—Reply. *Stat. Med.* **23**, 3242–3244 (2004).
- Matzka, J., Stolle, C., Yamazaki, Y., Bronkalla, O. & Morschhauser, A. The geomagnetic K_p index and derived indices of geomagnetic activity. *Space Weather* **19**, e2020SW002641 (2021).
- Alessio, E., Carbone, A., Castelli, G. & Frappietro, V. Second-order moving average and scaling of stochastic time series. *Eur. Phys. J. B* **27**, 197–200 (2002).
- Gu, G. F. & Zhou, W. X. Detrending moving average algorithm for multifractals. *Phys. Rev. E* **82** (2010).
- Djurovic, D. & Paquet, P. The common oscillations of solar activity, the geomagnetic field, and the earth’s rotation. *Sol. Phys.* **167**, 427–439 (1996).
- Hu, K., Ivanov, P. C., Chen, Z., Carpena, P. & Stanley, H. E. Effect of trends on detrended fluctuation analysis. *Phys. Rev. E* **64**, 011114 (2001).
- Hauke, J. & Kossowski, T. Comparison of values of Pearson’s and Spearman’s correlation coefficients on the same sets of data. *Quaest. Geographicae* **30**, 87–93 (2011).
- Box, G. E., Jenkins, G. M., Reinsel, G. C. & Ljung, G. M. *Time Series Analysis: Forecasting and Control* (John Wiley & Sons, 2015).
- Shen, Chenhua Analysis of detrended time-lagged cross-correlation between two nonstationary time series. *Phys. Lett. A* **379**, 680–687 (2015).
- Mukaka, M. M. Statistics Corner: a guide to appropriate use of Correlation coefficient in medical research. *Malawi Med. J.* **24**, 69–71 (2012).
- Savitz, D. A., Kristi-Anne, T. & Charles, P. Statistical significance testing in the American Journal of Epidemiology, 1970–1990. *Am. J. Epidemiol.* **139**, 1047–1052 (1994).
- Frigo, M. & Johnson, S. G. FFTW: An adaptive software architecture for the FFT. In *IEEE International Conference on Acoustics, Speech*

- and *Signal Processing (ICASSP 98)*. vol. 3, pp. 1381–1384 (IEEE, Seattle, WA, USA, 1998).
45. Torrence, C. & Compo, G. P. A practical guide to wavelet analysis. *Bull. Am. Meteorol. Soc.* **79**, 61–78 (1998).
 46. Jarque, C. M. & Bera, A. K. A test for normality of observations and regression residuals. *Int. Stat. Rev.* **55**, 163–172 (1987).
 47. El-Taher, A. M. & Thabet, A. A. The interconnection and phase asynchrony between the geomagnetic indices? periodicities: a study based on the interplanetary magnetic field polarities 1967–2018 utilizing a cross wavelet analysis. *Adv. Space Res.* **67**, 3213–3227 (2021).
 48. Cai, Y. Y. et al. Associations of short-term and long-term exposure to ambient air pollutants with hypertension a systematic review and meta-analysis. *Hypertension* **68**, 62 (2016).
 49. Lewington, S. et al. Seasonal variation in blood pressure and its relationship with outdoor temperature in 10 diverse regions of China: the China Kadoorie Biobank. *J. Hypertension* **30**, 1383–1391 (2012).
 50. Menvielle, M., Iyemori, T., Marchaudon, A. & Nosé, M. in *Geomagnetic Observations and Models* (eds Manda, M. & Korte, M.) (Springer Netherlands, 2011).
 51. Colafella, K. M. M. & Denton, K. M. Sex-specific differences in hypertension and associated cardiovascular disease. *Nat. Rev. Nephrol.* **14**, 185–201 (2018).
 52. Chu, Y. J., Wang, F. L. & Lou, Y. H. Epidemiological survey and analysis of perimenopausal symptoms in Qingdao. *Curr. Adv. Obstet. Gynecol.* **21**, 553–556 (2012).
 53. Teng, Z. J., Zhan, Z. J., Xue, Q. M., Bao, X. H. & Tang, H. X. A epidemiological survey on health condition of perimenopausal women in Weihai region. *Matern. Child Health Care China* **26**, 4744–4747 (2011).
 54. Dimitrova, S. Cardio-vascular homeostasis and changes in geomagnetic field, estimated by Dst-index. In *2nd International Conference on Electromagnetic Field, Health and Environment (EHE 2007)*. (Krawczyk, A. et al.) (IOS Press, 2007).
 55. Vieira, C. L. Z. et al. Geomagnetic disturbances driven by solar activity enhance total and cardiovascular mortality risk in 263 US cities. *Environ. Health* **18** (2019).
 56. Hao, J. W. & Lu, E. Variation of relative humidity as seen through linking water vapor to air temperature: an assessment of interannual variations in the near-surface atmosphere. *Atmosphere* **13** (2022).
 57. Brook, R. D. et al. Insights into the mechanisms and mediators of the effects of air pollution exposure on blood pressure and vascular function in healthy humans. *Hypertension* **54**, 659–667 (2009).
 58. Houck, P. D., Lethen, J. E., Riggs, M. W., Gantt, D. S. & Dehmer, G. J. Relation of atmospheric pressure changes and the occurrences of acute myocardial infarction and stroke. *Am. J. Cardiol.* **96**, 45–51 (2005).
 59. Marzouk, O. A. Assessment of global warming in Al Buraimi, sultanate of Oman based on statistical analysis of NASA POWER data over 39 years, and testing the reliability of NASA POWER against meteorological measurements. *Heliyon* **7** (2021).
 60. Bai, S. et al. Spatial distribution and semiannual variation of cold-dense plasma sheet. *J. Geophys. Res.-Space Phys.* **123**, 464–472 (2018).
 61. Cliver, E. W., Kamide, Y. & Ling, A. G. Mountains versus valleys: semiannual variation of geomagnetic activity. *J. Geophys. Res.-Space Phys.* **105**, 2413–2424 (2000).
 62. Russell, C. T. & McPherron, R. L. Semiannual variation of geomagnetic activity. *J. Geophys. Res.* **78**, 92–108 (1973).
 63. Palmer, S. J., Rycroft, M. J. & Cernack, M. Solar and geomagnetic activity, extremely low frequency magnetic and electric fields and human health at the Earth's surface. *Surv. Geophys.* **27**, 557–595 (2006).
 64. Alabdulgader, A. A. Space and human consciousness: the great whisper. *Nat. Sci.* **13**, 235–253 (2021).
 65. Cherry, N. Schumann resonances, a plausible biophysical mechanism for the human health effects of Solar/Geomagnetic activity. *Nat. Hazards* **26**, 279–331 (2002).
 66. Saroka, K. S., Vares, D. E. & Persinger, M. A. Similar spectral power densities within the schumann resonance and a large population of quantitative electroencephalographic profiles: supportive evidence for Koenig and Pobachenko. *PLoS ONE* **11** (2016).
 67. Babayev, E. S. & Allahverdiyeva, A. A. Effects of geomagnetic activity variations on the physiological and psychological state of functionally healthy humans: some results of Azerbaijani studies. *Adv. Space Res.* **40**, 1941–1951 (2007).
 68. Mitsutake, G. et al. Does Schumann resonance affect our blood pressure? *Biomedicine Pharmacother.* **59**, S10–S14 (2005).
 69. Mulligan, B. P. & Persinger, M. A. Experimental simulation of the effects of sudden increases in geomagnetic activity upon quantitative measures of human brain activity: validation of correlational studies. *Neurosci. Lett.* **516**, 54–56 (2012).
 70. Cornelissen, G. et al. Circasemiannual chronomics: half-yearly biospheric changes in their own right and as a circannual waveform. *Biomed. Pharmacother.* **57**, 45S–54S (2003).
 71. Portela, A. et al. Metachronanalysis of circannual and circasemiannual characteristics of human suprachiasmatic vasopressin-containing neurons. *Vivo (Athens, Greece)* **9**, 347–358 (1995).
 72. He, P. Potential influence of geomagnetic activity on blood pressure statistical fluctuations at mid-magnetic latitudes (v1.0). *Zenodo* <https://doi.org/10.5281/zenodo.14912276> (2025).

Acknowledgements

The authors would like to express our gratitude to the GFZ German Research Centre for Geosciences for the publicly available geomagnetic data. We are equally grateful to the China Weather Network, the Ministry of Ecology and Environment of the People's Republic of China, and the Weihai Municipal Ecological Environment Bureau for the publicly available environmental data. Our sincere thanks also go to Qilu Hospital of Shandong University (Qingdao) and Weihai Municipal Hospital for providing the blood pressure data. This work was supported by the National Natural Science Foundation of China (Nos. 42225405, 42350710200, and 42275135), the Shandong Provincial Government “Double Hundred” (WSR2023038), the Interdisciplinary Cultivation Program at Shandong University, Weihai, and the Science and Technology Development Fund, Macau SAR (File No. SKL-LPS(MUST)-2021-2023).

Author contributions

Q.S. and H.Z. designed the study. C.L., X.Z., and Y.Z. summarized the blood pressure data. P.H., C.L., M.X., R.G., C.H., Q.S., and H.Z. analyzed the data. P.H. and C.L. wrote the manuscript. All authors discussed the results and commented and edited the manuscript.

Competing interests

The authors declare no competing interests.

Additional information

Supplementary information The online version contains supplementary material available at <https://doi.org/10.1038/s43856-025-00822-w>.

Correspondence and requests for materials should be addressed to Huanhu Zhang or Quanqi Shi.

Peer review information *Communications Medicine* thanks the anonymous review for their contribution to the peer review of this work. [Peer reviewer reports are available].

Reprints and permissions information is available at <http://www.nature.com/reprints>

Publisher's note Springer Nature remains neutral with regard to jurisdictional claims in published maps and institutional affiliations.

Open Access This article is licensed under a Creative Commons Attribution-NonCommercial-NoDerivatives 4.0 International License, which permits any non-commercial use, sharing, distribution and reproduction in any medium or format, as long as you give appropriate credit to the original author(s) and the source, provide a link to the Creative Commons licence, and indicate if you modified the licensed material. You do not have permission under this licence to share adapted material derived from this article or parts of it. The images or other third party material in this article are included in the article's Creative Commons licence, unless indicated otherwise in a credit line to the material. If material is not included in the article's Creative Commons licence and your intended use is not permitted by statutory regulation or exceeds the permitted use, you will need to obtain permission directly from the copyright holder. To view a copy of this licence, visit <http://creativecommons.org/licenses/by-nc-nd/4.0/>.

© The Author(s) 2025